Early Steps of Supported Bilayer Formation Probed by Single Vesicle Fluorescence Assays

Joseph M. Johnson,* Taekjip Ha,† Steve Chu,† and Steven G. Boxer*
Departments of *Chemistry and †Physics, Stanford University, Stanford, California 94305-5080 USA

ABSTRACT We have developed a single vesicle assay to study the mechanisms of supported bilayer formation. Fluorescently labeled, unilamellar vesicles (30–100 nm diameter) were first adsorbed to a quartz surface at low enough surface concentrations to visualize single vesicles. Fusion and rupture events during the bilayer formation, induced by the subsequent addition of unlabeled vesicles, were detected by measuring two-color fluorescence signals simultaneously. Lipid-conjugated dyes monitored the membrane fusion while encapsulated dyes reported on the vesicle rupture. Four dominant pathways were observed, each exhibiting characteristic two-color fluorescence signatures: 1) primary fusion, in which an unlabeled vesicle fuses with a labeled vesicle on the surface, is signified by the dequenching of the lipid-conjugated dyes followed by rupture and final merging into the bilayer; 2) simultaneous fusion and rupture, in which a labeled vesicle on the surface ruptures simultaneously upon fusion with an unlabeled vesicle; 3) no dequenching, in which loss of fluorescence signal from both dyes occur simultaneously with the final merger into the bilayer; and 4) isolated rupture (pre-ruptured vesicles), in which a labeled vesicle on the surface spontaneously undergoes content loss, a process that occurs with high efficiency in the presence of a high concentration of Texas Red-labeled lipids. Vesicles that have undergone content loss appear to be more fusogenic than intact vesicles.

INTRODUCTION

Supported lipid bilayers are useful in vitro mimics for natural biological membranes. They can be used to model cell-cell interactions (Grakoui et al., 1999; Sackmann, 1996; Brian and McConnell, 1984) and for various biotechnological applications (Groves et al., 1997; Boxer, 2000). Supported bilayers consist of a continuous fluid bilayer of lipids that is held near a surface, typically glass or SiO_2, by a balance of van der Waals and hydration forces.

Vesicle fusion is one of the most convenient ways of creating supported lipid bilayers. The process of bilayer formation via vesicle fusion is interesting from a fundamental biophysical point of view and may also help us in understanding the features of related phenomena such as membrane fusion mediated by fusion proteins. In addition, a better understanding of the bilayer formation process may also provide guidance in the choice and preparation of the surfaces and in optimization of vesicle size and conditions for robust bilayer formation.

The fundamental processes of vesicle fusion and rupture in forming supported bilayers are usually depicted as in Fig. 1: *vesicle fusion* is the mixing of lipids between vesicles to form a larger, product vesicle and *vesicle rupture* is the conversion of a vesicle to a supported bilayer disk, accompanied by the loss of interior content. Additional processes may occur such as hemi-fusion, the mixing of outer leaflet lipids of two vesicles while contents remain separated (Lentz and Lee, 1999). Additionally, the interior content of a vesicle may be lost through a rupture pore without the vesicle being converted to a bilayer disk (i.e., leakage). Unless otherwise noted, in this paper "vesicle fusion" will be used to denote both full fusion and hemi-fusion events,

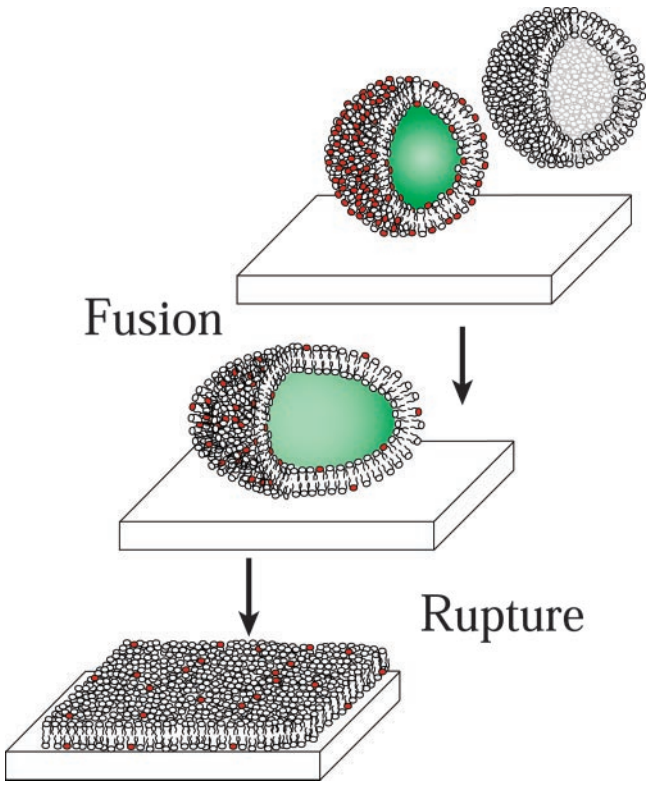

FIGURE 1 Proposed bilayer formation schematics. Adsorbed vesicles fuse among themselves until a critical size is reached, then rupture to form bilayer disks. TR fluorophores are shown in red and entrapped CF is shown in green.

Submitted June 5, 2002, and accepted for publication August 29, 2002.

Address reprint requests to Steven G. Boxer, Dept. of Chemistry and Physics, Stanford University, Stanford, CA 94305. E-mail: sboxer@stanford.edu.

0006-3495/02/12/3371/09 $2.00

while "vesicle rupture" will be used to represent both full conversion to a bilayer disk and simple content loss. When possible, distinctions will be made between hemi versus full fusion, and partial versus full rupture.

There has been important theoretical work regarding the shapes of vesicles both in solution and on a solid surface (Seifert and Lipowsky, 1990; Lipowsky and Seifert, 1991; Seifert, 1997), reviewed by Reviakine et al. (Reviakine and Brisson, 2000). For the purpose of this theory discussion, fusion and rupture are used in their fundamental sense (see Fig. 1). Seifert and Lipowsky suggested that the rupture of an adsorbed vesicle is size-dependent: if the vesicle is smaller than a critical size, it will not rupture. An energetic balance between favorable adhesion interactions and unfavorable line tension of the resulting bilayer disk determines the critical size. The time scale for fusion of small unilamellar vesicles in solution is considered to be on the order of hours ($k = 0.0017\ h^{-1}$ for DMPC vesicles at 36°C) (Lentz et al., 1987). However, the fusion rate is predicted to be enhanced by adsorption to a surface (Lipowsky and Seifert, 1991). Therefore, bilayer formation via vesicle fusion is expected to depend on the vesicle size and is thought to occur in four steps: single vesicle adsorption, fusion of vesicles on the surface to form larger vesicles, rupture of these vesicles to form bilayer disks on the surface, and final merging of the disks. Adsorption is essentially an irreversible process and is diffusion-controlled (Kam and Boxer, 2000). If the adsorbed vesicle is below the critical size, it will remain intact on the surface. Contact with another intact vesicle will result in fusion. This process will continue until the vesicle becomes larger than the critical size, at which point the vesicle ruptures to form a bilayer disk. Eventually, merger of the isolated bilayer disks will result in complete bilayer coverage of the surface.

There has also been important experimental work that monitored the supported membrane formation processes. Keller and co-workers used the Quartz Crystal Microbalance (QCM) and Surface Plasmon Resonance (SPR) to demonstrate the adsorption of intact vesicles up to a coverage of ~15% of the total lipid mass of a supported bilayer, at which point vesicle rupturing begins (Zhdanov et al., 2000; Keller and Kasemo, 1998; Keller et al., 2000). Reviakine et al. used atomic force microscope (AFM) imaging to show that the critical radius (R_c) for vesicle rupture on mica was between 50 and 100 nm. Both groups of investigators demonstrate that vesicles with $R < R_c$ remain intact on the surface. Muresan and Lee used AFM imaging to visualize shape changes in adsorbed vesicles, demonstrating the effect of line tension (Muresan and Lee, 2001). However, neither QCM/SPR nor AFM was able to directly detect the sequence of events involving vesicle fusion and rupture; the former technique measures bulk properties while the latter has limited time resolution.

It was our goal to directly observe vesicle fusion and rupture events at the single vesicle level to avoid ensemble averaging and to capture the multi-step processes of vesicle fusion, rupture, and extended bilayer formation with sufficient time resolution. We prepared vesicles labeled with a high concentration of Texas Red-labeled lipids (TR) and with encapsulated Carboxy Fluorescein dyes (CF) as a cargo, allowing visualization of single vesicles. By measuring both colors at the same time, both fusion and rupture events can be observed. A similar strategy is widely used in the membrane fusion literature (Chanturiya et al., 1997; McNew et al., 2000; Weber et al., 1998). Due to the limitations of our experiment, we were unable to distinguish hemi-fusion from full-fusion or partial rupture (i.e., pore formation) from full rupture (bilayer disk formation), except in some limiting cases. The term "fusion" will be used generically to refer to hemi- and full-fusion and it will be explicitly noted when differentiating between the two is possible. Similarly, the term "rupture" will be used generically to refer to both full and partial rupture, except when explicitly noted.

We begin with a sparse coverage of labeled vesicles adsorbed to the surface and then flow in unlabelled vesicles. An *observation zone* is defined around each adsorbed, labeled vesicle (see below). During the course of an experiment, the integrated intensities for the observation zone are independently recorded for red TR and green CF fluorescence. When the effective areal concentration of the fluorescent lipids decreases upon fusion between a labeled vesicle and an unlabeled vesicle, an increase in red TR fluorescence is observed due to the decrease in fluorescence self-quenching (dequenching); however, the green fluorescence for encapsulated CF persists. When a vesicle ruptures either transiently or permanently, fluorescence of CF disappears. Finally, upon merging into the large-scale bilayers, a rapid decrease in TR intensity is observed due to lateral diffusion and mixing of TR-lipids with unlabeled lipids outside the observation zone. By using an intensified CCD camera, wide-field fluorescence microscopy with total internal reflection excitation, and an in situ flow system, we can observe signatures associated with each of these pathways with video-rate time resolution.

MATERIALS AND METHODS

Materials

Egg phosphatidylcholine (Egg PC) and dioleoyl phosphatidylserine (DOPS) were purchased from Avanti Polar Lipids (Alabaster, AL). Texas Red 1,2-dihexadecanoyl-*sn*-glycero-3-phosphoethanolamine, triethylammonium salt (TR), 5-(and-6)-carboxyfluorescein mixed isomers (CF), and Alexa Fluor 647 carboxylic acid, succinimidyl ester (Alexa 647) were purchased from Molecular Probes (Eugene, OR). S65T-GFP (Q80R) expressed in *Escherichia coli*/ pRSET$_b$GFP/*N*-terminal polyhistidine purification tag was provided by Dr. Federico Rossell.

Vesicle preparation

Extruded unilamellar vesicles (referred to simply as vesicles) were prepared according to the protocol described in Rex (1996). Briefly, chloroform was evaporated from the egg PC by vacuum, and the lipids were then allowed to hydrate in standard buffer (10 mM Tris [pH 8], 100 mM NaCl). The resulting multilamellar vesicles were put through five freeze/thaw cycles and then extruded through polycarbonate membranes of 30-, 50-, or 100-nm pore diameter (Avanti Mini-Extruder). For labeled vesicles, TR was mixed with egg PC in chloroform; the mixture was dried and resuspended in a solution of the dye to be encapsulated. Aqueous dye solutions contained either 20 mM CF, 10 mM Alexa 647, or 1–2 mM GFP dissolved in 10 mM Tris [pH 8] buffer with the appropriate amount of NaCl to make the solution iso-osmolar (intravesicular solution: 20 mM CF, 10 mM Tris [pH 8] equilibrated with 50 mM NaOH, 65 mM NaCl) with the standard buffer. Vesicles were generally prepared at a nominal lipid concentration of ~5 mg/ml, and subsequently diluted before experiments. TR-labeled vesicles with encapsulated dyes were separated from external dyes by eluting through a Sepharose CL-4B column (40–165 μm) equilibrated with standard buffer (extravesicular solution: 10 mM Tris [pH 8], 100 mM NaCl). Vesicles were generally used within one day of preparation, and external dyes were removed on the day of the experiment. The lipid concentration in vesicle solutions was checked by converting lipid phosphate into an inorganic form, and then colorimetrically determining the concentration (Prasad, 1996). The lipid content of all labeled and unlabeled vesicle solutions was found to be ~6 mg/ml.

Bulk fluorescence measurements

Bulk fluorescence measurements were used to determine how much the TR signal would increase by dequenching when an unlabeled vesicle fuses with a labeled vesicle of the same size. Vesicle solutions of 0.5%, 1%, 3%, and 6% TR with and without 20 mM CF were diluted to an absorbance of 0.05 OD at the CF absorption maximum for vesicles with CF or at the TR absorption maximum for vesicles without CF. The necessary dilution for each solution varied linearly with mole-percent of TR incorporated, indicating that vesicles containing up to 6% TR lipids can be prepared with the full incorporation of the expected amount of TR. Fluorescence measurements were then performed in a quartz cuvette using a fluorimeter and exciting at 540 nm for vesicles without CF and 488 nm for vesicles with CF.

Substrate preparation

Quartz substrates were used for samples studied under flow. These were cleaned by sequential sonication in detergent solution, water, acetone, ethanol, 1 M potassium hydroxide solution, and water. Experiments to determine the fraction of pre-ruptured vesicles were performed on glass and quartz surfaces prepared either using the method described above or by soaking the substrates in heated detergent solution, followed by rinsing and baking at 400°C for 4 h, with identical results.

Microscopy

For measurements performed under flow conditions, we used the prism-based, total internal reflection (TIR) excitation method on a Nikon TE300 inverted microscope with a 60× water immersion objective. An argon ion laser was used for excitation (488 nm, 0.05 mW/50 μm^2) and a Pentamax Gen IV CCD camera was used to obtain the images at the rate of 30 frames/s. The experimental set-up has in situ automated flow capabilities. Data analysis was performed with home-written software. The details of the experimental set-up have been previously published (Zhuang et al., 2000). The labeled vesicles were diluted in the standard buffer to a lipid concentration of 83 ng/ml, and 100 μl was then injected into quartz flow cells to obtain an approximate surface concentration of 1 vesicle per 200 μm^2. The vesicles were allowed to adsorb for ~5 min, and then the flow cell was washed with standard buffer. To initiate bilayer formation, various dilutions (0.625–2.5 mg/ml) of unlabeled egg PC vesicles were delivered continuously (12 μl/s) and the data were recorded until the bilayer homogeneously covered the surface. There is a 4.5-s delay from the time that the flow is initiated until vesicles arrive at the observation area, due to the dead volume. An observation zone of 2 μm diameter was defined around each labeled vesicle, and the integrated intensities were recorded within each observation zone for both red and green fluorescence. A 498-nm long-pass filter was used to reject the laser excitation light, and a pair of 550-nm long-pass dichroic filters were used to split the red and green fluorescence into separate paths that were detected on the two halves of the CCD camera.

To determine the fraction of vesicles showing encapsulated dye signals, some samples were examined on a separate TE300 microscope using epi-illumination with a 100× oil immersion objective and standard Chroma filter sets to distinguish colors. Finally, to determine whether vesicles underwent a cargo loss while in solution, a confocal microscope was used with Ar 488-nm and HeNe 543-nm laser illumination.

RESULTS AND DISCUSSION

Adsorption of vesicles

Individual 50 nm diameter vesicles prepared with 6% TR-labeled lipids and encapsulated CF were examined first in solution to be certain that TR and entrapped CF were both present. This was done using a confocal fluorescence microscope by observing vesicles that diffused through the excitation volume in solution. A correlation was seen between intensities of TR and CF emission for each individual vesicle, signified by a burst of fluorescence signal, and all vesicles appeared to contain CF. These vesicles were then adsorbed to a quartz support at low surface coverage. Fig. 2 shows a dual view image (integration of 30 frames) of adsorbed vesicles: the fluorescent spots on the left side are due to the encapsulated CF, while the spots on the right side are due to TR. The average CF signal intensity is ~25% of the average TR signal. A schematic illustration of one observation zone (radius = 2 μm) is shown. It is apparent from the image that ~50% of the vesicles detected by TR fluorescence have no corresponding spot detected on the CF side. Because each vesicle in solution exhibited both TR and CF fluorescence, the absence of CF fluorescence is attributed to pre-ruptured vesicles that ruptured in isolation upon adsorption to the quartz surface before observation began. A salt concentration of 50–200 mM NaCl was necessary for adsorption of vesicles with 6% TR. Adsorbed vesicles were stable on the time scale of an hour if left undisturbed in the dark. No motion or change, other than gradual photobleaching, was observed from the vesicles in control experiments where buffer containing no vesicles was passed through the flow cell.

Bulk bilayer formation

The rate of bilayer formation was determined by measuring the time delay between the initial exposure of surface-

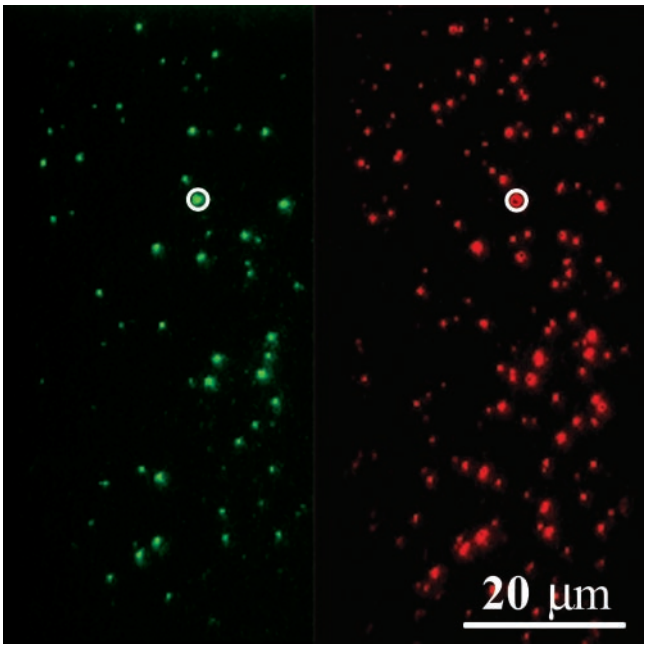

FIGURE 2 False color image of the average of the first 30 frames (1 s) of fluorescence images from labeled vesicles (50 nm diameter) adsorbed to a surface. The contrast and brightness for each half have been adjusted independently to aid visualization. Illustrative examples of circular observation zones (2 μm diameter) are shown surrounding one vesicle on each half of the image.

adsorbed vesicles to various concentrations (0.625–2.5 mg/ml) of unlabeled vesicles (12 μl/s flow rate) and the final bilayer formation as signified by the decay of TR fluorescence. The final bilayer formation time was determined by averaging all the TR traces and by determining the half-point of TR decay. A linear relationship between the bilayer formation rate and the lipid concentration (hence vesicle concentration) was observed, with a proportionality constant of $\sim$0.1 s^{-1} ml/mg. This is consistent with the previous observation by Keller et al. (2000) that the bilayer formation is governed by the exposure of the surface to vesicles (vesicle concentration $\times$ time).

Primary fusion

Bilayer formation was initiated by flowing in 0.625 mg/ml of unlabeled vesicles, and the time evolution of the fluorescence intensities of labeled vesicles for each observation zone were monitored. Fig. 3 *A* shows an example trace in which TR dequenching occurs before CF intensity decrease. Dequenching signals are expected to occur when a labeled vesicle on the surface fuses with an unlabeled vesicle(s), causing the dilution of the lipid-conjugated dyes. From the bulk fluorescence measurements of various concentrations of lipid-conjugated dyes (data not shown), we would expect that the fluorescence intensity of a labeled vesicle (6% TR) would increase by a factor of $\sim$2 upon fusion with one unlabeled vesicle of the same size, which is consistent with the signal change in Fig. 3 *A*. The initial fusion occurs without the loss of CF, hence the resulting *product* vesicle remains intact. It should be noted that it is not possible to distinguish whether hemi-fusion or full fusion is observed in Fig. 3 *A*. The concentration of CF used (20 mM) is reported to be >40% quenched in vesicles (Schwarz and Arbuzova, 1995); however, no dequenching was observed in the CF

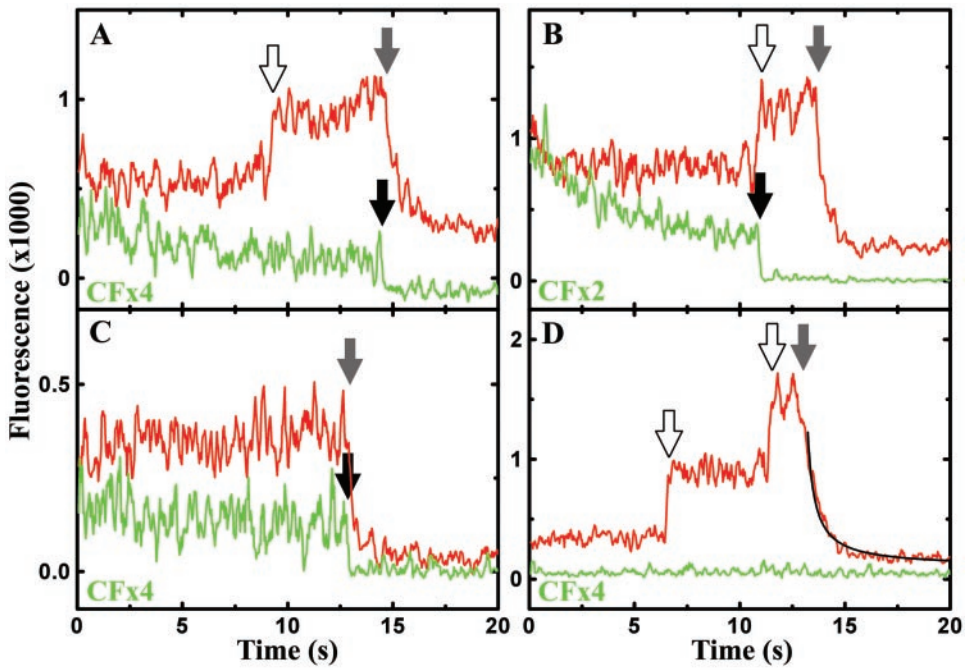

FIGURE 3 Examples of four dominant pathways observed during bilayer formation (50 nm diameter vesicles, labeled containing 6% TR (*red*) and 20 mM CF (*green*) and unlabeled flowed in at 0.625 mg/ml). Data were smoothed by adjacent 5-point averaging. Arrows indicate distinct bilayer formation events: clear arrows correspond to dequenching, gray incorporation into bulk bilayer, and black to rupture. (*A*) Primary fusion comprises 8% of the pathways observed for all vesicles (CF signal multiplied by 4 to aid visualization). (*B*) Simultaneous fusion and rupture (12%, CFx2). (*C*) No dequenching (25%, CFx4). (*D*) Pre-rupture (50%, CFx4). A fit (see text and Appendix 1) with a diffusion coefficient of 2 $\mu m^2/s$ is shown. The remaining 5% of pathways were observed isolated rupture (data not shown).

signal. Lack of CF dequenching could indicate that hemi-fusion is responsible for TR dequenching, and full fusion only occurs concomitantly with rupture. However, it is also possible that lack of CF dequenching is due to photobleaching of CF. The observed loss of CF emission 6 s later is interpreted as rupturing. At the same time, the TR intensity begins to decrease to a final equilibrium value. This reduction is interpreted as the diffusion of TR-lipids out of the 2-μm-diameter observation zone once the ruptured vesicle has been connected to a bilayer patch significantly larger than the observation zone. Because the loss of CF intensity is concomitant with the beginning of decrease in TR signal, it appears that the loss of CF is caused by the complete rupture of the vesicle and subsequent incorporation into an extended area of planar bilayer. This type of trace was one of four types consistently observed, and is referred to as primary fusion. In all cases, unavoidable photobleaching causes a steady reduction in the average amplitude of the TR and CF fluorescence, sometimes obscuring transitions.

Simultaneous fusion and rupture

Fig. 3 *B* shows an example trace of a vesicle in which TR fluorescence increase and CF decrease occur simultaneously. This is interpreted as the rupture (partial or complete) of the adsorbed vesicle as soon as it fuses with another unlabeled vesicle, and is referred to as simultaneous fusion and rupture. It is not possible to tell absolutely if hemi- or full-fusion occurs during TR dequenching. It seems improbable that hemi-fusion would accompany rupture, as a high energy pore must be created even for partial rupture, which would favor full fusion if in contact with another vesicle.

No dequenching

Fig. 3 *C* shows an example trace of a vesicle that shows no dequenching, but does show simultaneous disappearance of TR and CF signals when the vesicle merges with the large-scale bilayer. It is likely that the labeled vesicle is incorporated directly into a bilayer patch significantly larger than the observation area, and the diffusion of the TR out of the observation zone occurs so rapidly that no dequenching signal is observed. The gradual decrease in TR signal argues against the possibility that the labeled vesicle is desorbed from the surface.

Isolated rupture

Fig. 3 *D* shows an example trace of a vesicle in which no CF fluorescence is observed. Presumably, the vesicle underwent isolated rupture (either partial or complete) on the surface before observation began. This type of pre-rupturing occurs for ~50% of the adsorbed vesicles (see Fig. 2). This vesicle shows a 2-step increase in TR fluorescence due to dequenching, presumably from the successive fusion events with incoming, unlabeled vesicles, and then eventual decay of TR fluorescence due to diffusion out of the observation zone and mixing with unlabeled lipids. The decrease in TR fluorescence can be fit assuming a Gaussian distribution of the fluorescent area that widens as time passes, and from this a diffusion coefficient on the order of 1 $\mu m^2/s$ can be extracted for the TR lipids (see Appendix 1). This is consistent with diffusion coefficients previously measured for lipids in a supported bilayer (Groves and Boxer, 1995; Kung et al., 2000; Stelzle et al., 1992; Schutz et al., 1997). Isolated rupture traces were fit to determine diffusion coefficients (to avoid interference in the decay from dequenching or loss of CF).

Determining the causes for isolated rupture

To test whether the high dye content (6% TR) is responsible for vesicle pre-rupturing, vesicles containing 0.5% TR and 20 mM CF were prepared. The same protocol was used for this experiment as was used for experiments with 6% TR: a small amount of labeled vesicles were allowed to adsorb to the surface, the flow cell was rinsed with buffer, and then a 0.625 mg/ml solution of unlabeled vesicles was flowed through. Only 8% of the vesicles (50 and 100 nm diameter) underwent isolated pre-rupture under these conditions, that is, almost all adsorbed vesicles exhibited both TR and CF signals. Upon addition of unlabeled vesicles, no TR dequenching signal was expected (due to the negligible initial self-quenching) or observed. It was found that when the TR signal decreased, the CF signal decreased simultaneously for all adsorbed vesicles observed, that is, all traces were similar in appearance to the traces in Fig. 3 *C*. This led us to conclude that 6% TR is able to induce the pre-rupture and enhance the fusogenicity of adsorbed vesicles. With 0.5% TR, no rupture is observed before reduction of the TR signal, indicating that vesicles merge with bilayer patches significantly larger than the observation zone.

TR may cause vesicles to pre-rupture either through electrostatics (TR is negatively charged) or through steric effects. To differentiate between the two, vesicles were prepared that contained 0.5% TR and 5.5% DOPS, a negatively charged lipid (50 nm diameter). Only ~16% isolated content loss was observed for these vesicles, which suggests that electrostatics do not play a major role in TR-induced isolated content loss.

There are several possible mechanisms for the apparent pre-rupturing: 1) vesicles have undergone full rupture to form small supported bilayer disks; 2) some vesicles undergo partial rupture (i.e., leakage) when in contact with the surface, allowing exchange of the entrapped dye with bulk buffer, but not forming bilayer disks, and 3) unknown interactions between the dyes (possibly self-quenching of CF or energy transfer from CF to TR) can cause quenching

of the CF signal. To probe the effects of interactions among dyes, we prepared 100-nm vesicles that contained 6% TR and encapsulated GFP. Approximately 50% of these vesicles were also pre-ruptured. The chromophore of GFP is contained within a protein barrel, which should protect it from dye-dye quenching. In addition, experiments performed with encapsulated Alexa 647 and 6% TR vesicles (50 nm diameter) also show ~50% pre-rupturing rate. These experiments argue against a dye-dye quenching interaction that is specific to CF (see Appendix 2). It also demonstrates that loss of interior dye signal cannot be due to energy transfer to TR, as the emission peak of Alexa 647 is 83 nm to the red of the excitation peak of TR. This suggests that mechanism 3 does not apply here. To differentiate between mechanisms 1 and 2, AFM experiments were performed on samples with the same composition and prepared under similar conditions. Only intact vesicles, no bilayer disks, were found (Schonherr et al., manuscript in preparation). This leaves mechanism 2 as the most likely scenario. Because even GFP is able to leak out of some adsorbed vesicles via a partial rupture, the pore formed during the leakage must be greater than ~3 nm. Peptide-induced leakage of vesicles has been shown to be modulated by osmotic induced membrane tension (Polozov et al., 2001). It is possible that the combination of TR and membrane tension induced by adsorption to the surface (Lipowsky and Seifert, 1991) may cause similar leakage.

Bilayer formation pathways

Here we summarize the different pathways observed for vesicle fusion and rupture during bilayer formation. For the 6% TR 20 mM CF vesicles studied in the greatest detail, it was found that ~50% underwent pre-rupture, as depicted in Fig. 3 *D*, and ~25% of the vesicles showed no dequenching, as depicted in Fig. 3 *C*. The remaining ~25% of the traces followed pathways depicted in Fig. 3, *A* or *B* (plus a small amount that underwent isolated rupture—see below) and are summarized in Fig. 4. Fig. 4 shows a histogram of the time delay Δt (defined as the time between CF disappearance time and *initial* TR dequenching) for individual 50 nm diameter vesicles that showed both TR dequenching and CF signal. The histogram is divided into three regions corresponding to three different pathways of bilayer formation. Vesicles with Δt values greater than 0 follow the primary fusion pathway (Fig. 3 *A*), in which vesicles first undergo fusion to form larger vesicles and then rupture at a later time. Vesicles with $\Delta t \sim 0$ correspond to a pathway of simultaneous fusion and rupture (Fig. 3 *B*). A very small number of vesicles (~5%) had Δt values less than 0, which corresponds to isolated rupture *while under observation* (an example trace for this is not shown). Table 1 summarizes the statistics of bilayer formation pathways obtained for 30-, 50-, and 100-nm diameter vesicles that show both TR dequenching and CF signal. We considered vesicles

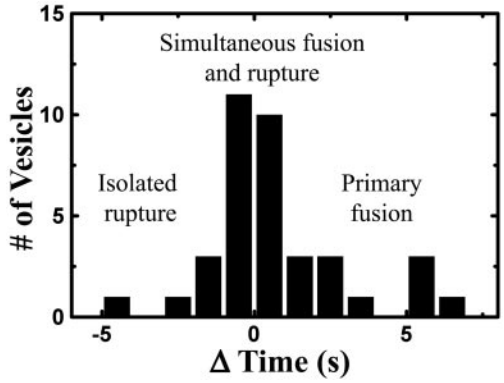

FIGURE 4 A histogram of the time delay Δt, defined as the time between initial fusion (dequenching of TR signal) and rupture (loss of CF), from the experiment described in Fig. 3.

with $\Delta t < -0.5$ s or $\Delta t > 0.5$ s as having undergone isolated rupture or primary fusion, respectively. For all vesicle sizes studied, ~50% appear to undergo simultaneous fusion and rupture, while primary fusion is slightly less common and isolated rupture is the least common pathway.

Nucleation efficiency of pre-ruptured versus intact vesicles

Are pre-ruptured vesicles more effective in catalyzing vesicle fusion? To answer this question, we first grouped the vesicles into two classes, intact and pre-ruptured. For each class of vesicles we determined the initial and final transition times. The initial transition is defined as either the first TR signal increase due to dequenching or a decrease in fluorescence due to final merging to a large-scale bilayer if the dequenching is not observed. The final transition is defined as the decay of TR signal due to the final merging with the bilayer. Fig. 5 shows histograms of the initial (*left*) and final (*right*) TR transition times for intact (*top*) and pre-ruptured (*bottom*) vesicles. Both classes of vesicles (intact versus pre-ruptured) exhibit approximately the same final transition times, which is consistent with the idea that final transition times indicate when bulk bilayer coverage is achieved. However, the initial transitions for pre-ruptured

TABLE 1 Percentage of vesicles undergoing different decomposition pathways

	30-nm Vesicles	50-nm Vesicles	100-nm Vesicles
Number of vesicles containing CF with TR dequenching	17	37	40
Primary fusion (Fig. 3 *A*)	41%	32%	37.5%
Simultaneous fusion and rupture (Fig. 3 *B*)	53%	49%	55%
Isolated rupture (trace not shown)	6%	19%	7.5%

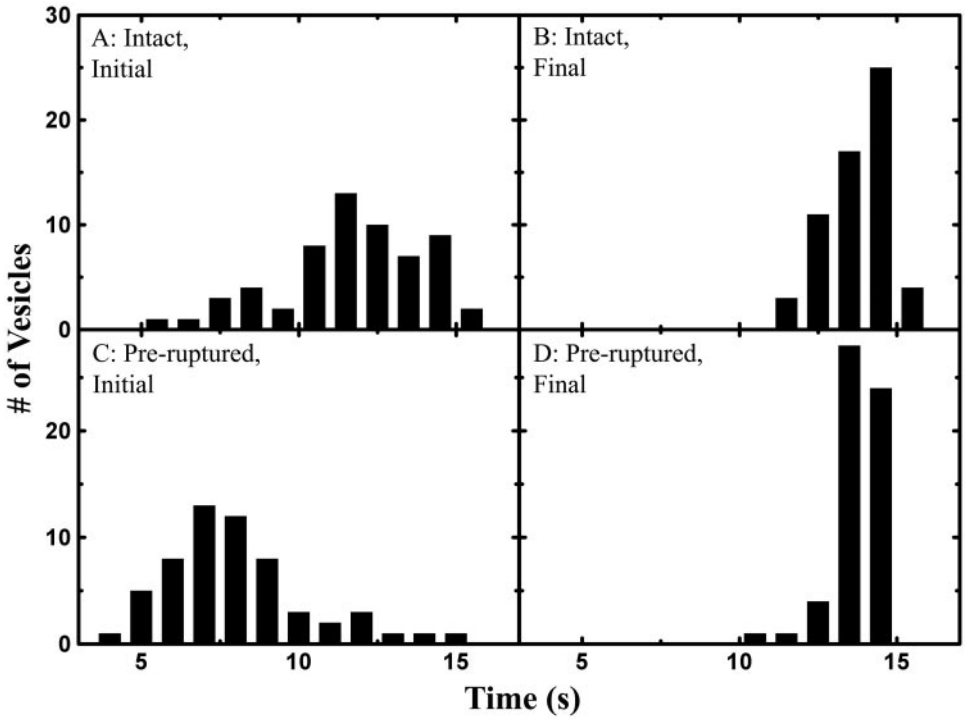

FIGURE 5 Histograms for intact vesicles of the initial (*A*) and final (*B*) transition times (defined in the text) and for pre-ruptured vesicles (*C*, *D*). The final transitions for intact and pre-ruptured vesicles appear to occur around the same time. The initial transitions for pre-ruptured vesicles occur consistently earlier than those of intact vesicles.

vesicles occur earlier than the initial transitions for intact vesicles, indicating that the pre-ruptured vesicles are more likely to participate in the earlier phase of supported bilayer formation.

Is the enhanced fusogenicity of pre-ruptured vesicles intrinsic or simply the result of "hot" spots on the surface that induce rupture of the incoming vesicles? The experiments described below show that vesicles that were osmotically induced to rupture showed fusogenic behavior similar to pre-ruptured vesicles, arguing against site-specific surface effects; 100-nm-diameter vesicles containing 6% TR and 20 mM CF were adsorbed in high salt solution (200 mM). Millipore water was then flowed through the sample cell, and 100% of the adsorbed vesicles were observed to rupture (loss of CF). This type of osmotically induced content loss has been previously observed for vesicles in contact with black lipid membranes (Chanturiya et al., 1997). The high salt buffer was restored and a solution of 0.625 mg/ml of unlabeled vesicles was then flowed in under the same buffer conditions. Nearly all traces showed dequenching, and histograms of initial and final transitions times looked qualitatively similar to the histograms in Fig. 5 for pre-ruptured vesicles (data not shown). In particular, there were a significant number of early initial TR changes (relative to the final TR transition times) for the osmotically ruptured vesicles. AFM measurements were also performed on adsorbed vesicles subjected to osmotic shock, and it was found that some, but not all, vesicles were induced to rupture completely (i.e., to form bilayer disks, see Appendix 2). Thus, it appears that osmotic shock caused some vesicles to completely rupture and some to partially rupture (i.e., leakage occurs).

The histograms of initial transition times for both populations of vesicles were separated into two approximately Gaussian-shaped distributions, one corresponding to early changes and one corresponding to late changes. Table 2 shows the percent of vesicles showing early time changes [(number of early transitions)/(number of early + number of late)] for both intact vesicles and pre-ruptured vesicles, for all vesicle sizes examined. Independent of vesicle size, pre-ruptured vesicles showed a larger percentage of early transitions.

The observation that pre-ruptured vesicles show more early TR transitions than intact vesicles indicates that pre-ruptured vesicles have an increased ability to induce fusion and rupture of incoming vesicles. A similarity between pre-ruptured and osmotically ruptured vesicles is that they are both farther along the reaction path to supported bilayer formation; pre-ruptured vesicles have already undergone

TABLE 2 Percentage of vesicles showing early transitions

	30-nm Vesicles	50-nm Vesicles	100-nm Vesicles
Intact vesicle	8%	17%	18%
Pre-ruptured vesicle	22%	81%	75%
100% Osmotically pre-ruptured vesicle	N.D.	N.D.	88%

% early = [(number of early transitions)/(number of early + number of late)] × 100 (see Fig. 7).

content loss and fully ruptured vesicles are already bilayer disks. Perhaps pre-ruptured and osmotically ruptured vesicles have already overcome an activation barrier to bilayer formation, making them more fusogenic. It is possible that "fusion" from these states is not typical of fusion depicted in Fig. 1. When a bilayer disk, or a vesicle with a "rupture pore" comes into contact with an incoming vesicle, they may transition directly into a bilayer disk with area $8\pi r^2$, instead of undergoing traditional fusion.

Using QCM and SPR, Keller et al. observed that vesicles are stable on the surface until a "threshold density" is achieved, at which point conversion from adsorbed vesicles into a supported bilayer takes place (Keller and Kasemo, 1998; Keller et al., 2000). Using AFM, Reviakine et al. also observed intact vesicles below a certain critical radius, and were able to estimate the critical radius for rupture on mica as 50–100 nm (Reviakine and Brisson, 2000). The work from both groups suggests that fusion is a precursor to rupture of vesicles on the surface. We also observed intact, isolated vesicles that were stable on the surface. In addition, we observed fusion and subsequent rupture events, which showed variation in their order and timing. In some cases, we observed isolated content loss but not formation bilayer disks, demonstrating the fluctuating nature of vesicles adsorbed to a surface. We did not observe strong size dependence in the fusion or rupture behavior of the vesicles. High TR content caused ~50% pre-rupturing rate independent of size within the size range studied. Increased fusogenicity was observed for both partially and fully ruptured vesicles.

APPENDIX 1

Fit to determine diffusion constant

The solution for Fick's 2nd law from a point source into two dimensions is

$$C(t, x, y) = C_0/(4PiDt) \cdot \exp[-(x^2 + y^2)/4Dt] \quad \text{(A1)}$$

in which $C(t, x, y)$ is the concentration as a function of time and space and D is the diffusion coefficient (Crank, 1986). In the data collection, a Gaussian weighting function, $\exp[-0.4(x^2 + y^2)]$, is applied over the observation zone. We make the assumption that $C(t, x, y)$ combined with the weighting function is negligible outside of the observation zone (due to the weighting function). Integrating the combined function over all space, and assuming that the concentration combined with the weighting function gives the observed intensity I', we find

$$I'(t) = I_0/[1.6D(t - t_0)] + I'' \quad \text{(A2)}$$

Here t_0 is a time offset included to adjust for the variable decay time of TR curves and I'' is an intensity background value to adjust for the variable TR value at $t = \infty$. The diffusion coefficient D is in units of pixel^2/s, and must be converted by the ratio of μm^2/pixel^2 = 0.6.

APPENDIX 2

Texas Red photophysics

It was found that the fluorescence of TR-labeled vesicles shifted to the blue upon photobleaching. Thus TR vesicles (without CF) that were bleached through a standard Chroma TR filter set became visible through a Chroma FITC filter set. This photoconversion was further confirmed by experiments done in bulk solution, in which TR-labeled vesicles were bleached with 540 (20) nm light and studied in a conventional fluorimeter. It was found that the excitation and emission of the TR shifted to the blue by 15–20 nm. To ensure that this artifact not cause CF emission of dual-labeled vesicles to be overestimated, photobleaching of TR was kept to a minimum. A similar phenomenon has been observed in Bodipy 581/591, and has been utilized as a ratiometric assay for lipid oxidation (Pap et al., 1999); however, we could find no similar information on Texas Red.

We thank Dr. Peter Lentz and Dr. Steven Andrews for extensive helpful discussions.

This work was supported in part by a grant from the NSF Biophysics Program and by the CPIMA MRSEC Program of the NSF under award DMR-9808677. S. Chu was supported by an NSF grant in Polymers and Biophysics.

REFERENCES

Boxer, S. G. 2000. Molecular transport and organization in supported lipid membranes. *Curr. Opin. Chem. Biol.* 4:704–709.

Brian, A. A., and H. M. McConnell. 1984. Allogenic stimulation of cytotoxic T cells by supported planar membranes. *Proc. Natl. Acad. Sci. U.S.A.* 81:6159–6163.

Chanturiya, A., L. V. Chernomordik, and J. Zimmerberg. 1997. Flickering fusion pores comparable with initial exocytotic pores occur in protein-free phospholipid bilayers. *Proc. Natl. Acad. Sci. U.S.A.* 94: 14423–14428.

Crank, J. 1986. The Mathematics of Diffusion. Oxford University Press, New York.

Grakoui, A., S. K. Bromley, C. Sumen, M. M. Davis, A. S. Shaw, P. M. Allen, and M. L. Dustin. 1999. The immunological synapse: a molecular machine controlling T cell activation. *Science.* 285:221–227.

Groves, J. T., and S. G. Boxer. 1995. Electric-field-induced concentration gradients in planar supported bilayers. *Biophys. J.* 69:1972–1975.

Groves, J. T., N. Ulman, and S. G. Boxer. 1997. Micropatterning of fluid lipid bilayers on solid supports. *Science.* 275:651–653.

Kam, L., and S. G. Boxer. 2000. Formation of supported lipid bilayer composition arrays by controlled mixing and surface capture. *J. Am. Chem. Soc.* 122:12901–12902.

Keller, C. A., K. Glasmastar, V. P. Zhdanov, and B. Kasemo. 2000. Formation of supported membranes from vesicles. *Phys. Rev. Lett.* 84:5443–5446.

Keller, C. A., and B. Kasemo. 1998. Surface specific kinetics of lipid vesicle adsorption measured with a quartz crystal microbalance. *Biophys. J.* 75:1397–1402.

Kung, L. A., L. Kam, J. S. Hovis, and S. G. Boxer. 2000. Patterning hybrid surfaces of proteins and supported lipid bilayers. *Langmuir.* 16: 6773–6776.

Lentz, B. R., T. J. Carpenter, and D. R. Alford. 1987. Spontaneous fusion of phosphatidylcholine small unilamellar vesicles in the fluid phase. *Biochemistry.* 26:5389–5397.

Lentz, B. R., and J. K. Lee. 1999. Poly(ethylene glycol) (PEG)-mediated fusion between pure lipid bilayers: a mechanism in common with viral fusion and secretory vesicle release? (Review). *Mol. Membr. Biol.* 16:279–296.

Lipowsky, R., and U. Seifert. 1991. Adhesion of vesicles and membranes. *Molecular Crystals and Liquid Crystals.* 202:17–25.

McNew, J. A., F. Parlati, R. Fukuda, R. J. Johnston, K. Paz, F. Paumet, T. H. Sollner, and J. E. Rothman. 2000. Compartmental specificity of cellular membrane fusion encoded in SNARE proteins. *Nature.* 407: 153–159.

Muresan, A. S., and K. Y. C. Lee. 2001. Shape evolution of lipid bilayer patches adsorbed on mica: an atomic force microscopy study. *J. Phys. Chem. B.* 105:852–855.

Pap, E. H. W., G. P. C. Drummen, V. J. Winter, T. W. A. Kooij, P. Rijken, K. W. A. Wirtz, J. A. F. OpdenKamp, W. J. Hage, and J. A. Post. 1999. Ratio-fluorescence microscopy of lipid oxidation in living cells using C11-BODIPY581/591. *FEBS Lett.* 453:278–282.

Polozov, I. V., G. M. Anantharamaiah, J. P. Segrest, and R. M. Epand. 2001. Osmotically induced membrane tension modulates membrane permeabilization by class L amphipathic helical peptides: nucleation model of defect formation. *Biophys. J.* 81:949–959.

Prasad, R. 1996. Manual on membrane lipids. *In* Springer Lab Manual. Springer-Verlag, Berlin, Heidelberg.

Reviakine, I., and A. Brisson. 2000. Formation of supported phospholipid bilayers from unilamellar vesicles investigated by atomic force microscopy. *Langmuir*.16:1806–1815.

Rex, S. 1996. Pore formation induced by the peptide melittin in different lipid vesicle membranes. *Biophys. Chem.* 58:75–85.

Sackmann, E. 1996. Supported membranes: scientific and practical applications. *Science.* 271:43–48.

Schutz, G. J., H. Schindler, and T. Schmidt. 1997. Single-molecule microscopy on model membranes reveals anomalous diffusion. *Biophys. J.* 73:1073–1080.

Schwarz, G., and A. Arbuzova. 1995. Pore kinetics reflected in the dequenching of a lipid vesicle entrapped fluorescent dye. *Biochim. Biophys. Acta. Biomembr.* 1239:51–57.

Seifert, U. 1997. Configurations of fluid membranes and vesicles. *Adv. Phys.* 46:13–137.

Seifert, U., and R. Lipowsky. 1990. Adhesion of Vesicles. *Phys. Rev. A.* 42:4768–4771.

Stelzle, M., R. Miehlich, and E. Sackmann. 1992. 2-Dimensional microelectrophoresis in supported lipid bilayers. *Biophys. J.* 63:1346–1354.

Weber, T., B. V. Zemelman, J. A. McNew, B. Westermann, M. Gmachl, F. Parlati, T. H. Sollner, and J. E. Rothman. 1998. SNAREpins: minimal machinery for membrane fusion. *Cell.* 92:759–772.

Zhdanov, V. P., C. A. Keller, K. Glasmastar, and B. Kasemo. 2000. Simulation of adsorption kinetics of lipid vesicles. *J. Chem. Phys.* 112:900–909.

Zhuang, X. W., L. E. Bartley, H. P. Babcock, R. Russell, T. J. Ha, D. Herschlag, and S. Chu. 2000. A single-molecule study of RNA catalysis and folding. *Science.* 288:2048–2051.